Supplementary Data

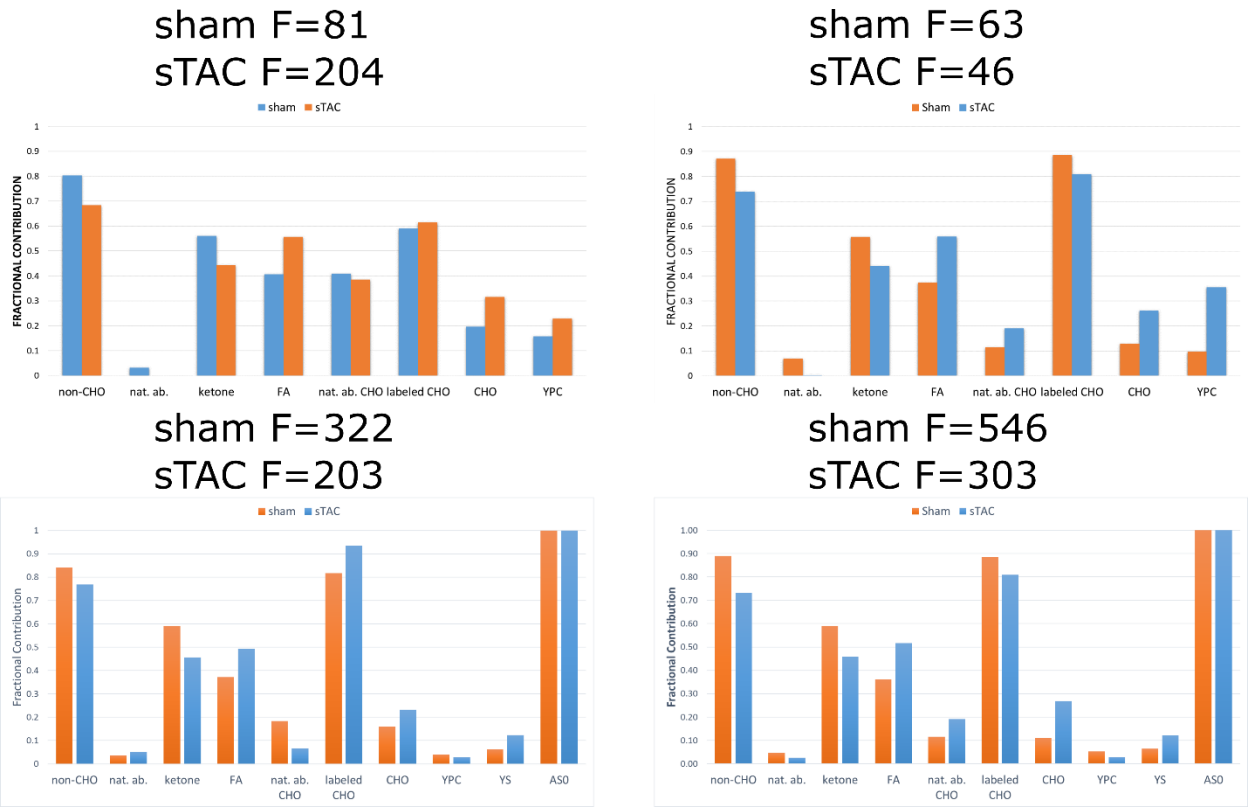

Figure S1. Summary of fractional contributions of various pathways to intermediary metabolism in sham surgeries (n=8) versus the sTAC (n=7) surgery. The x-axis labels from left to right denote non-carbohydrate (non-CHO) contributions to acetyl-CoA as compared to flux through PDH, the natural abundance fraction of non-CHO contributions, the fraction of ketones as a proportion of the non-CHO contributions, the fraction of fatty acids as a proportion of the non-CHO contributions, natural abundance CHO contributions, labeled CHO contributions, the fraction of PDH flux that accounts for all acetyl-CoA (CHO), pyruvate anaplerosis (Ypc), anaplerosis through succinyl-CoA of glutamate (Ys), and the fraction of Ys that arises from unlabeled substrate (AS0). The F-values report the goodness of fit for the simulation compared to the data. The reported F-values are the average values for all experiments. (Top left) Pyruvate anaplerosis, no fractional enrichment constraint. (Top right) Pyruvate anaplerosis with fractional enrichment of the carbohydrate precursor pool constrained to alanine enrichment. (Bottom left) Anaplerosis though pyruvate *and* succinate, no fractional enrichment constraint. (Bottom right) Anaplerosis though pyruvate *and* succinate, including fractional enrichment of carbohydrate precursor pool set to that of alanine. Note that the worst F-value is achieved when using the alanine enrichment and the model lacking Ys (top right) and the best F-value is achieved when including Ys and the fractional enrichment of alanine as a proxy of the carbohydrate pool enrichment. Using the fractional enrichment of lactate instead of alanine produced marginally worse fits.

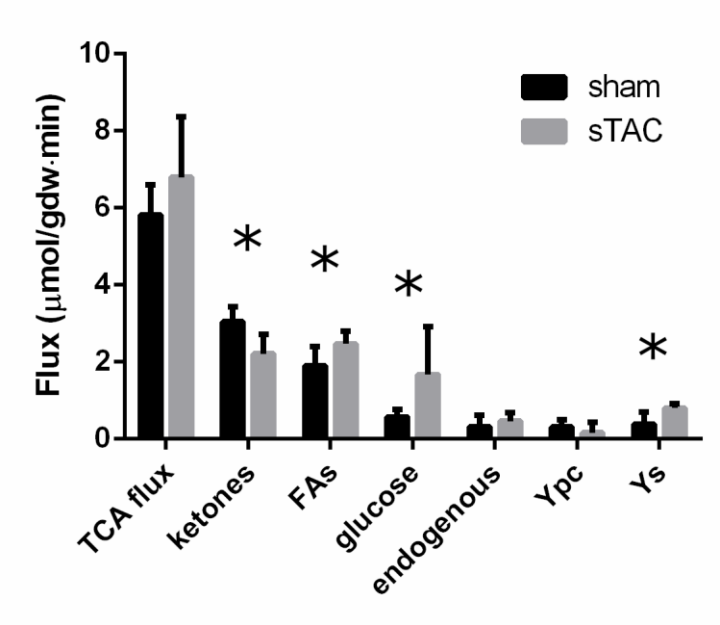

Figure S2. Absolute oxidative and anaplerotic flux for sham (n=8) and sTAC (n=7) perfused hearts. When normalized to O_2 consumption, ketone, fatty acid, and glucose oxidation are all significantly different, with increments in FA and glucose oxidation replacing ketone oxidation as fractions of TCA turnover. However, ketone oxidation is very high initially, which is likely due to the use of acetoacetate as a tracer. Estimates of anaplerotic flux, either via pyruvate carboxylation or through succinate, do not depend directly on acetoacetate as a tracer. With known loss of cardiac efficiency in HF, the equivalence between O_2 consumption and TCA cycle turnover is likely not preserved. Therefore, the absolute flux estimates here are likely incorrect, as the assumptions used to produce this figure are not enforceable. However, the detection of increased flux through Ys is not subject to this limitation, as it is based only on the isotopomer data.

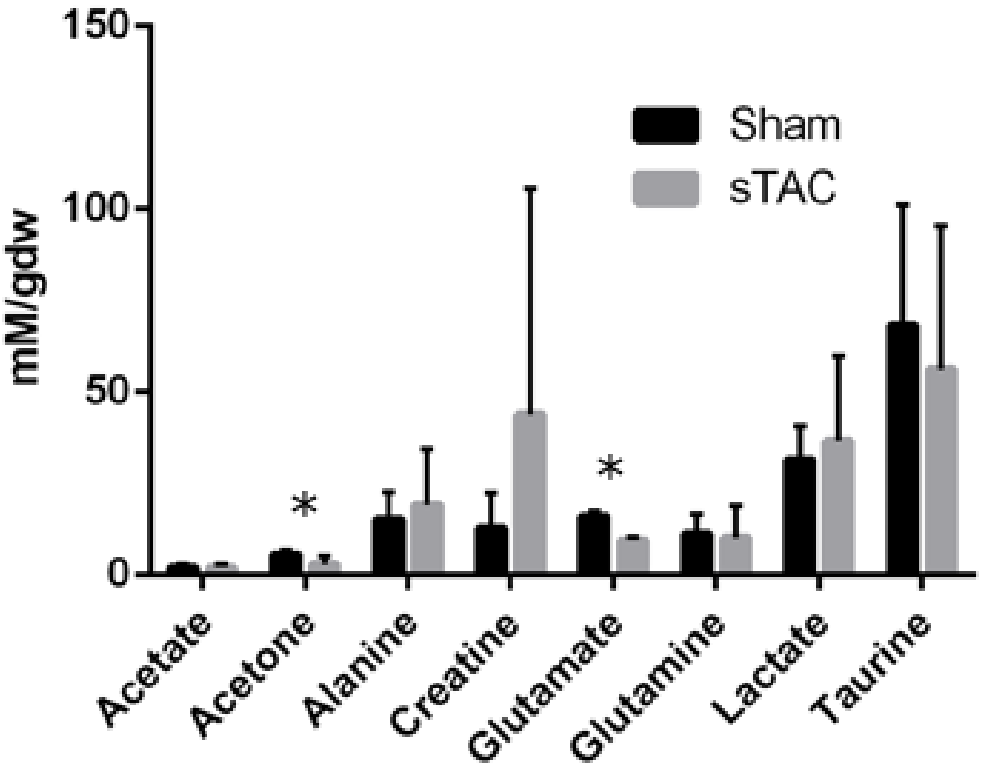

Figure S3. ^{1}H NMR metabolomics of the sham hearts (n=8) and sTAC hearts (n=7) also used for the ^{13}C analysis. The creatine is not significantly different between groups because of 2 outliers in the sTAC model. However, glutamate is significantly lower in sTAC, while glutamine is unchanged. Acetone, a breakdown product of acetoacetate and β-hydroxybutyrate was significantly decreased in sTAC.

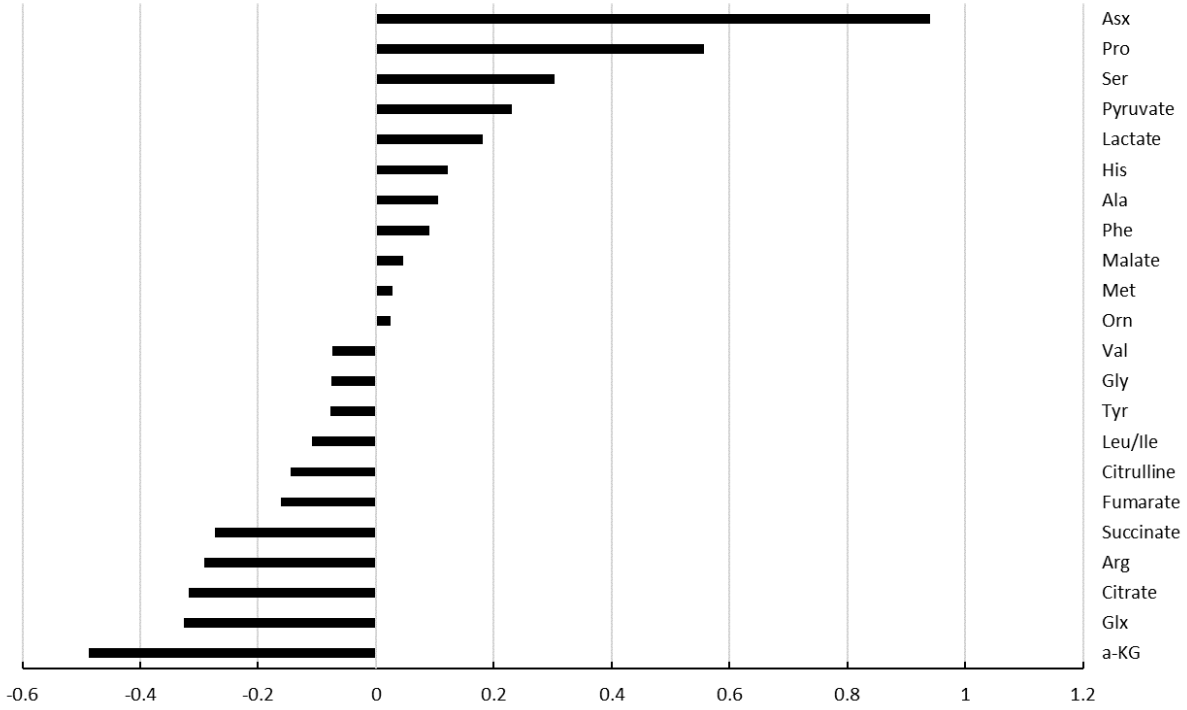

Figure S4. Fold change analysis of sham (n=6) versus sTAC mice (n=5) for organic and amino acids taken from the hearts of mice immediately sacrificed, not after perfusion. Log-base-2 scaled values of the LC/MS peak intensities were used. Negative values are downregulated in sTAC. Only α-ketoglutarate was significantly different after FDR correction. Note that while succinate is not significantly different, it is decreased, not increased. If ketone oxidation were upregulated, succinate would likely be increased because of its use as a co-factor by OXCT1.

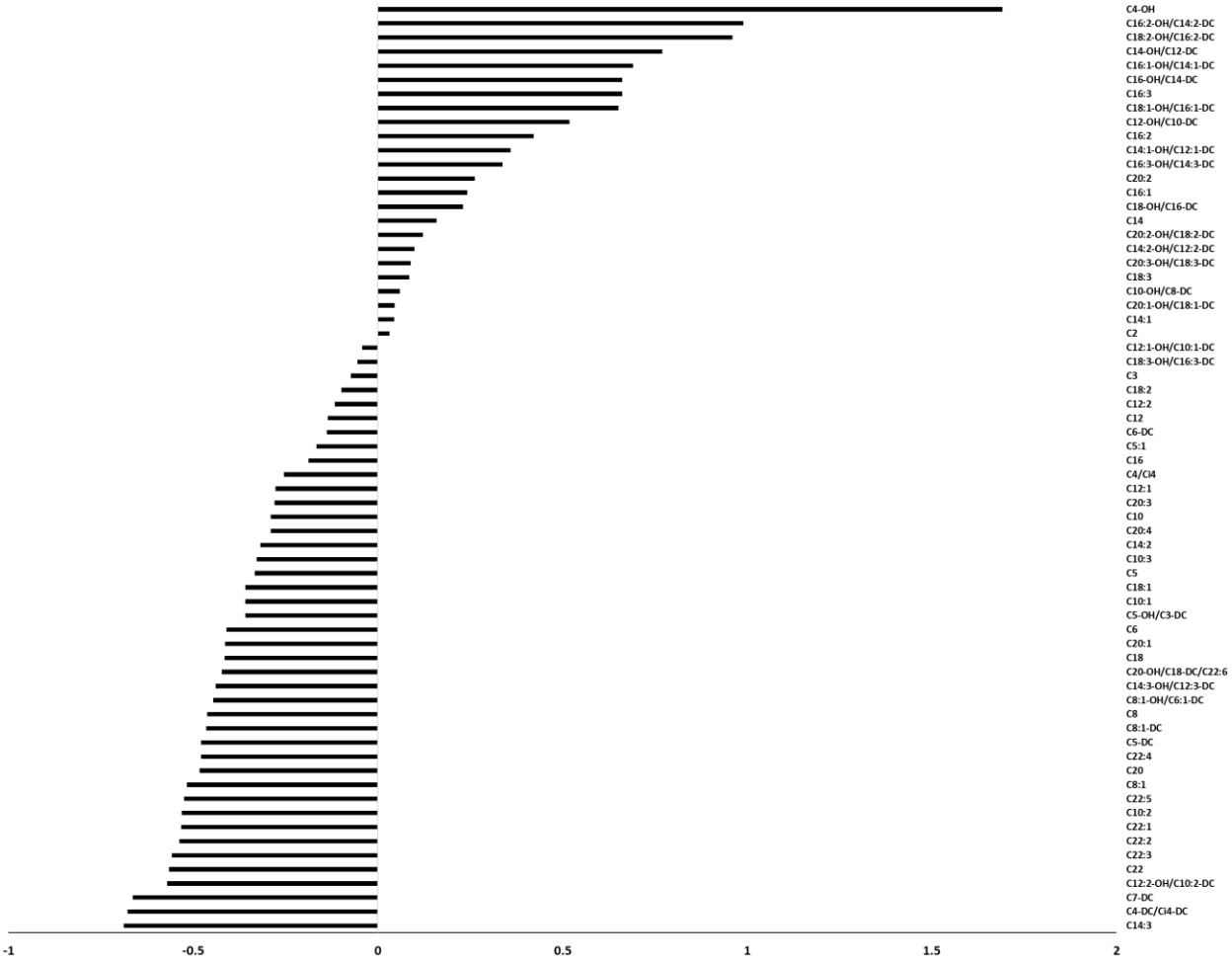

Figure S5. Fold change analysis of sham (n=6) versus sTAC (n=5) mice for acylcarnitines. Log-base-2 scaled values of the LC/MS peak intensities were used. Negative values are downregulated in sTAC. Despite the appearance of strong trends in the data, no significant differences were detected using multiple t-tests with FDR correction at 0.05. β-hydroxybutrylcarnitine (C4-OH, top)) showed a change in excess of 2-fold, but was driven by a single result.

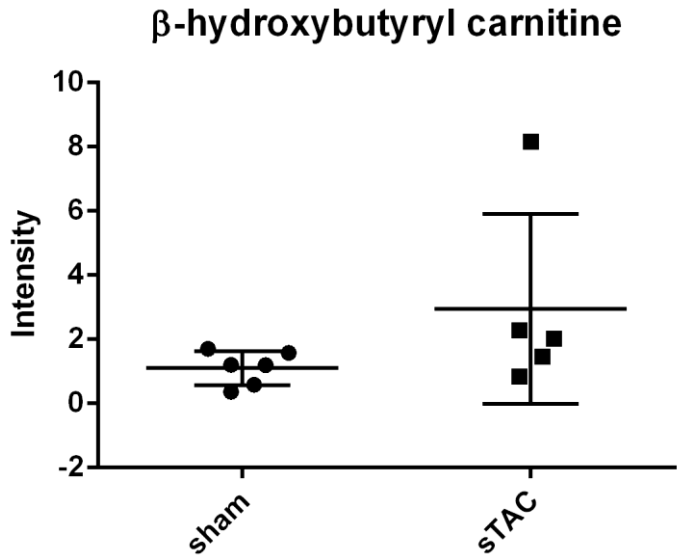

Figure S6. Differences in the β-hydroxybutyryl carnitine were driven by a single sample that was not chosen for exclusion from the whole panel, despite a very high response for this single metabolite.

Table S1. Echocardiographic parameters in SHAM, TAC 1wk, TAC 3wks and sTAC 1wk

	SHAM *(n=5)*	**TAC 1wk** *(n=5)*	**TAC 3wks** *(n=5)*	**sTAC 1wk** *(n=5)*
IVSd, mm	1.16±0.04	1.58±0.04*	1.44±0.02*	1.54±0.05*
IVSs, mm	1.74±0.05	2.04±0.05*	2.00±0.03*	1.76±0.04$^{\#}$
LVIDd, mm	2.46±0.05	2.42±0.04	2.53±0.04	3.44±0.17$^{*\#}$
LVIDs, mm	0.98±0.02	1.02±0.02	1.18±0.02*§	2.80±0.10$^{*\#}$
LVPWd, mm	0.88±0.02	1.14±0.05*	1.24±0.02*	1.08±0.10
LVPWs, mm	1.72±0.07	1.78±0.05	1.98±0.04*	1.28±0.10$^{*\#}$
EF, %	90.64±0.34	89.08±0.53	86.04±0.65*	33.86±2.43$^{*\#}$
FS, %	60.15±0.54	57.84±0.72	53.38±0.75*	18.31±1.74$^{*\#}$
LV mass, mg	80.35±0.97	128.70±6.61*	132.41±4.48*	191.56±9.64$^{*\#}$
HR, bpm	655±18.77	687±5.89	657±17.12	669±15.68

Data are expressed as mean±SEM

Abbreviations used: SHAM, sham-operated mice; **TAC**, transverse aortic constriction; **sTAC,** severe transverse aortic constriction; **1wk**, 1 week after surgery; **3wks**, 3 weeks after surgery; **IVSd**, end-diastolic interventricular septal wall; **IVSs**, end-systolic interventricular septal wall; **LVIDd,** left ventricular internal end-diastolic diameter; **LVIDs**, left ventricular internal end-systolic diameter; **LVPWd**, left ventricular end-diastolic posterior wall; **LVPWs**, left ventricular end-systolic posterior wall; **EF**, ejection fraction; **FS**, fractional shortening; **LV**, left ventricle; **HR**, heart rate; **mm**, millimetres; **mg**, milligrams; **bpm**, beats per minute; **SEM**, standard error of the mean. *p<0.01 vs. SHAM; §p<0.01 vs. TAC 1wk; $^{\#}$p<0.01 vs. TAC 1wk and TAC 3wks.